

STRUCTURE AND REACTIVITY IN ASYMMETRIC HYDROGENATION; A MOLECULAR GRAPHICS
ANALYSIS

JOHN M. BROWN AND PHILLIP L. EVANS

Dyson Perrins Laboratory, South Parks Rd. Oxford OX1 3QY, U.K.

(Received in UK 11 May 1988)

Summary: The crystallographic data available for chelate bisphosphine rhodium complexes have been evaluated. The origin of the widely-quoted "edge-face" arrangement in 5-ring chelates may lie in a stabilising interaction between *ortho* PCH groups and the coordinatively unsaturated metal; the tendency to assume this conformation is most marked when the chelate backbone is rigid. Using data derived for CHIRAPHOS complexes a simple molecular mechanics approach has been used to define the source of diastereoselectivity in dehydroamino acid binding to chiral rhodium bisphosphine entities, which resides in differential Van der Waals interactions between carboxyl and P-aryl groups for the two diastereomers. Their relative energy is reversed at the dihydride stage, following addition of H₂ to the bound enamide complex. Only one of the four possible stereoisomers in each diastereomeric family is viable; the rest suffer from substantial non-bonding interactions. Addition of H₂ to both enamide complexes in the CHIRAPHOS series was also studied through this molecular modelling approach. The minor enamide experiences substantial repulsive interactions in the early stages of reaction, but much less than the major enamide as Rh-H bond formation approached completion.

The asymmetric hydrogenation of dehydroamino acids and their structural relatives continues to stimulate interest, through both preparative¹ and mechanistic² studies. Whilst the basic principles which lead to high enantioselectivity are reasonably well understood, and the catalytic cycle is broadly defined in at least one case^{3,4}, much remains to be learned. In particular, the origin of enantioselectivity at the rate-determining transition-state, in which H₂ adds to the rhodium enamide complex, is unknown. It is generally recognised that the thermodynamically disfavoured enamide complex reacts more rapidly with H₂, and this event may be observed at low temperatures; under such conditions the putative dihydride breaks down faster than it is formed, and only an alkylhydride is seen⁵. Kagan has proposed⁶ the general rule that bisphosphine rhodium chelates of λ configuration give rise to *S*-amino acid on catalytic hydrogenation (and, by implication, $\delta + R$). There are no exceptions, but the rule is empirical and lacks support at the molecular level.

Since experimental work leading to characterisation of the initially formed dihydride had been unsuccessful⁷, we turned attention to computer modelling as a means of probing this inaccessible but crucial area of the energy surface.

RESULTS AND DISCUSSION

1. Conformations from X-Ray Analyses

The vast majority of successful ligands for asymmetric hydrogenation are bisphosphines with four pendant aryl groups. There are about seventeen relevant X-ray crystal structures of rhodium bisphosphine complexes in the literature. On the basis of early work with DIPAMP complexes Knowles and co-workers suggested that the orientation of phenyl rings imposed by ligand chirality was responsible for stereochemical control in asymmetric hydrogenation⁸. Their X-ray structure suggested that two rings were edge-on to the metal, and two rings face-on with an overall C₂ symmetry; this edge-face array was given a central role in their discussion,

and it can be clearly seen in the crystal structure of the CHIRAPHOS complex displayed in plan and elevation in 2. (Figure 1,2) A subsequent careful analysis by Oliver and Riley⁹ was more pessimistic about the generality of the edge-face relationship, however.

We retrieved the atomic coordinates of all available chiral rhodium bisphosphine complexes via the CSSR data file ; where these had not been deposited they were retrieved by direct correspondence with the original authors. Conversion into orthogonal coordinates was carried out through the CRYSTALS programs.¹⁰ Two further structures of square-planar chiral bisphosphine complexes were included for completeness.

Conformational analysis of the data was carried out by assembling the values for two torsional angles, about P - Rh - P - C_{aryl} [ψ] and about Rh - P - C_{aryl} - C_{ortho} [θ]. The former expresses the orientation of the P-phenyl group with respect to the chelate ring (i.e. whether it is ψ -axial or ψ -equatorial) whereas the latter reveals torsion about the aryl-C bond (whether it is edge-on or face-on). Idealised arrangements are indicated in Figures 2a-e.

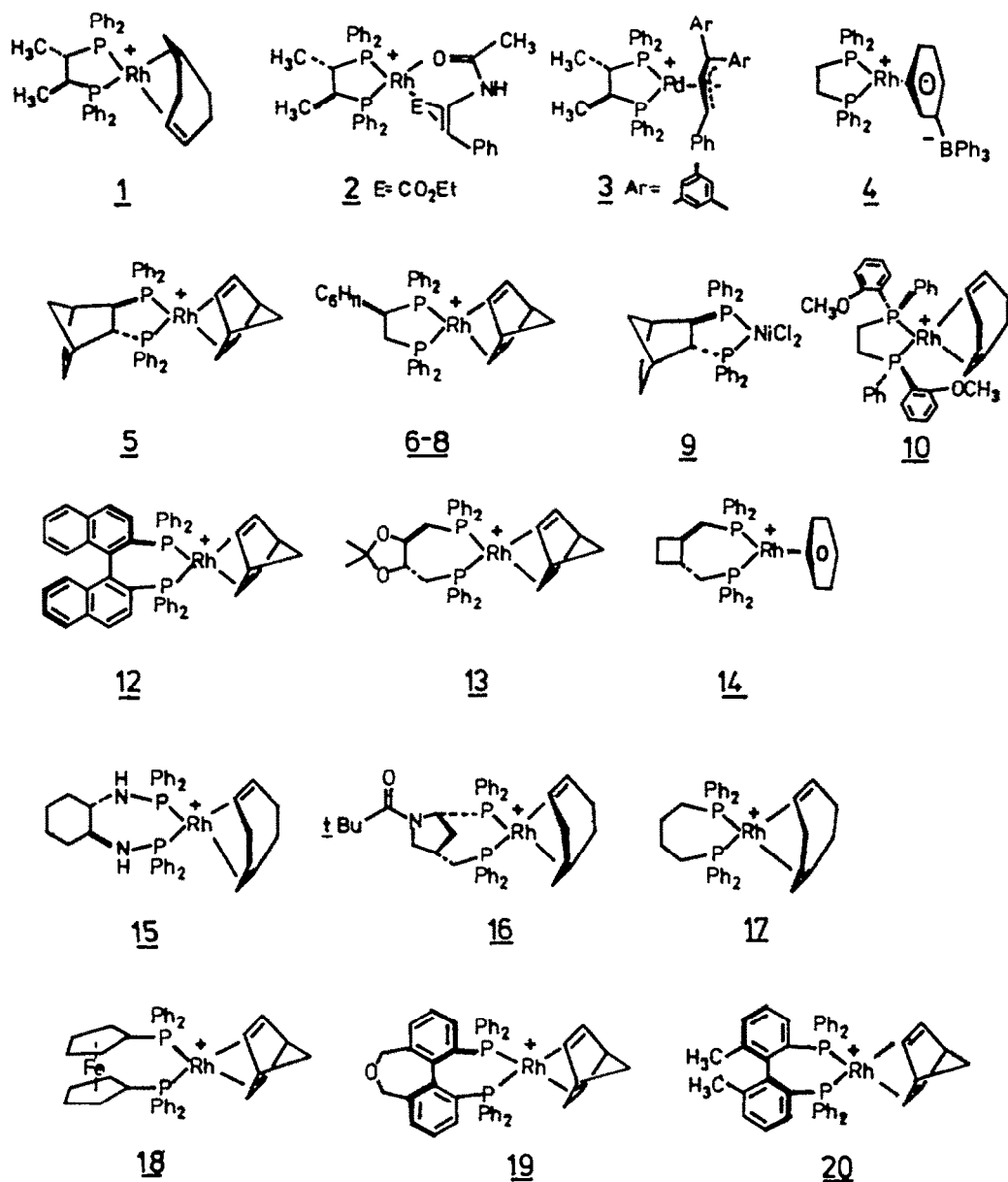


Figure 1 Structures 1-20 of Tables 1 and 2 (counterions to cations omitted)

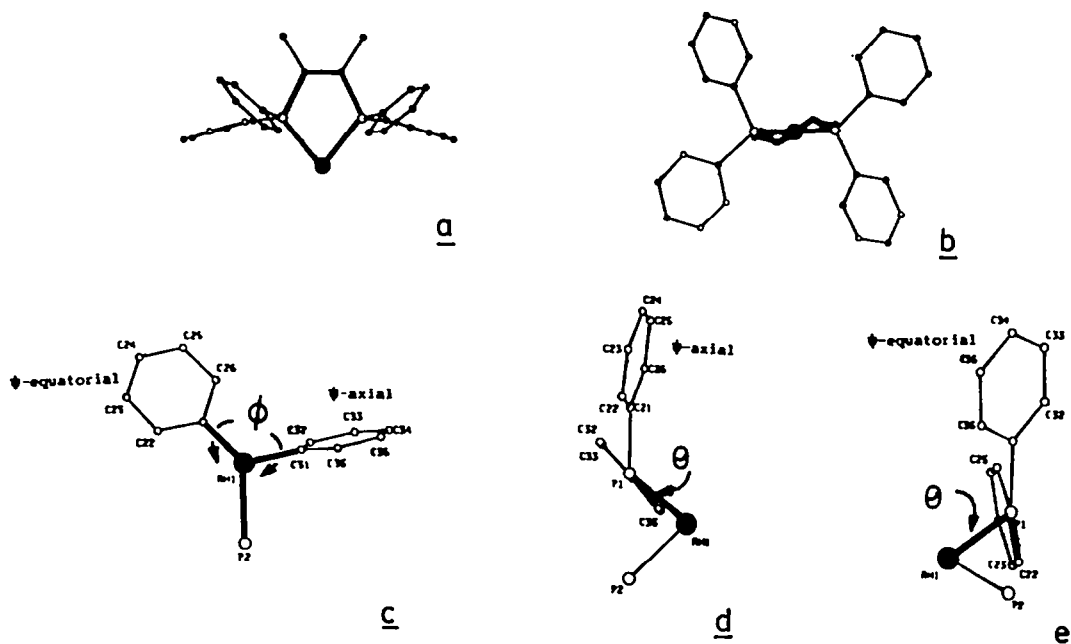


Figure 2 Views of chelate biphosphine structures. (a) Edge-face complex in plan (b) Edge-face complex in elevation (c) Torsion angles ϕ , viewing down Rh-P1 (d) Torsion angle θ for the edge-on ring, viewing down P1-C (ortho) (e) Torsion angle θ for the face-on ring, viewing down P1-C (ortho). Views (a) and (b) are taken from structure 2, the others are idealised.

Torsion angles: The torsion angle data displayed in Table 1 has been normalised to provide internal consistency and correlate structures of both absolute configurations. Firstly, the signs of torsion angle to rings A and C have been inverted for chelates of δ -configuration and the signs of torsion angle inverted for rings B and D in chelates of λ configuration. Secondly, the slight deviation from coplanarity in each pair of C-C (ortho) bonds was allowed for by taking an averaged torsional angle normalised for the one remote from its geminal P-Ph ring.

The plot of angles θ versus ϕ in Figure 3 reveals a definite tendency for clustering into ψ -axial and ψ -equatorial groups each with a rather narrow range of P-aryl orientations. For complexes 1-3 derived from the rigid ligand CHIRAPHOS, and related rigid complexes 5 and 9, together with that of the P-chiral bisphosphine DIPAMP 10, there is good agreement with the idealised edge-face arrangement of Figure 2. The edge-on ring is invariably ψ -axial and the face-on ring ψ -equatorial. For two of the three structural variants revealed in X-ray analysis of the CYCPHOS complex 6,8, the -PPh₂ entity adjacent to the cyclohexyl substituent conforms to the idealised edge-face arrangement, but the remote PPh₂ does not. The third structural variant 7 is anomalous and possess a non C₂- conformation of the five-membered chelate ring, as does the DIPHOS complex 4. These observations indicate that close conformity to idealised geometry is not a prerequisite for asymmetric catalysis, since CHIRAPHOS and CYCPHOS rhodium complexes demonstrate comparable optical efficiency in hydrogenation⁹. It seems that both carbons of the chelate backbone must possess equatorial substituents to achieve this idealised geometry - thereby imposing a symmetrical twist-conformation on the chelate which predisposes the P-aryl rings towards the C₂-symmetrical edge-face array.

Complex	Ring A		Ring B		Ring C		Ring D	
	θ°	$-\phi^\circ$	θ°	ϕ°	θ°	$-\phi^\circ$	θ°	ϕ°
1b	10	106	70	131	8	103	70	134
2c	19	102	87	136	21	106	83	132
3d	30	105	81	131	13	100	88	139
4e	71	116	24	122	26	92	69	142
5f	6	104	63	135	-7	100	43	132
6g	-14	107	85	134	76	113	27	124
7g	-26	114	67	126	28	95	52	136
8g	-4	103	68	136	66	105	-3	127
9h	11	107	86	127	0	98	70	132
10 ⁱ	3	104	75	137	23	98	66	140
11 ^a	0	100	70	130	0	100	70	130

Table 1 Torsion angle data derived from crystal structures 1 - 10, normalised as described in the text; Figure 2 provides a key. (a) Idealised values for the edge-face arrangement. (b) R.G. Ball and N.C. Payne *Inorg.Chem.* 16 (1977) 1187. (c) A.S.C. Chah, J.J. Pluth and J. Halpern, *J.Am.Chem.Soc.*, 102 (1980) 5952. (d) D.H. Farrar and M.C. Payne, *J.Am.Chem.Soc.*, 107 (1985) 2054. (e) P. Albano, M. Aresta and M. Marassero, *Inorg.Chem.*, 19 (1980) 1069. (f) E.P. Kyba, R.E. Davis, P.M. Juri and K.R. Shirley, *Inorg.Chem.*, 20, (1981) 3616. (g) Ref 11, main text; there are three independent molecules in the X-ray crystal. (h) H. Brunner, G. Vifulli, W. Porzio and M. Zocchi, *Inorg.Chim.Acta* 96 (1985) 67; this nickel complex has a PNIP angle of 90° (i) Ref 8, main text.

Complex	Ring A		Ring B		Ring C		Ring D	
	θ°	$-\phi^\circ$	θ°	ϕ°	θ°	$-\phi^\circ$	θ°	ϕ°
12 ^a	7	87	78	155	8	79	56	163
13 ^b	-1	90	81	150	12	103	81	139
14 ^c	3	108	85	177	58	142	16	101
15 ^d	48	70	76	174	-23	134	88	109
16 ^e	75	141	2	102	0	80	76	163
17 ^f	18	70	76	174	-23	127	82	113
18 ^g	65	142	16	99	-1	69	86	173
19 ^h	19	65	54	175	-2	102	47	138
20 ^h	+12	65	58	175	0	106	44	135

Table 2 Torsion angle data derived from crystal structures 12 - 20 (a) K. Toriumi, T. Ito, H. Takaya, T. Souchi and R. Noyori, *Acta Cryst* 38B (1982) 807. (b) R. Stults and W.S. Knowles, Monsanto, private communication. (c) J.M. Townsend and J.F. Blount, *Inorg.Chem.*, 20 (1981) 269. (d) K. Onuma and A. Nakamura, *Bull.Chem.Soc.Japan* 54 (1981) 761. (e) Y. Ohga, Y. Iitako, A.T. Kogure and I. Ojima, 25th Symposium on Organometallic Chemistry, Osaka, Japan 1978; Abstract 3A15. (f) M.P. Anderson and L.H. Pignolet, *Inorg.Chem.*, 20 (1981) 4101; (g) W.R. Cullen, T.-J. Kim, F.W.B. Einstein and T. Jones *Organometallics* 4 (1985) 346; (h) R. Schmid, M. Cereghetti, B. Heiser, P. Schonholzer and H.J. Hansen, *Helv.Chim.Acta* (1988) in press; G. Svensson, J. Albertsson, T. Frejd and T. Klingstedt, *Acta Cryst* C 42 (1986) 1324.

For 7-ring chelate complexes the position is less clear-cut. Of nine X-ray structures described (including one derived from a ferrocenylbiphosphine which has a comparable bite-angle) only two conform closely to the idealised C_2 -conformation of the chelate ring; both of these have the symmetrical edge-face arrangement of P-aryl rings. One is the rigid complex 12 derived from BINAP¹¹ and the other the related DIOP complex 13. Several further X-ray structures of organometallics bearing the DIOP ligand have been reported¹², and Kagan has undertaken a conformational analysis of the chelate ring geometry¹³. It is worth noting that complex 13 is the only DIOP-derived structure which approximates to C_2 symmetry in the twist-chair conformation. Several alternative low-energy conformations are available to the 7-ring chelate, this feature being apparent in the related complexes 14 - 17. Two of these conform rather well to cycloheptane twist-boat geometry¹⁴, namely 15 and 17; this is illustrated in Figure 4. This conformation characteristically places one P-Ph ring vector in the PRHP plane. Complexes 14 and 16 exhibit a similar orientation, and even the ferrocene-derived complex 18 shows this feature. The BINAP-related structure 19 based on the atropisomeric [3,4][5,6] dibenzooxepane ring system shows some deviation from ideal geometry, particularly in ring B. It is almost superimposable on the simpler biphenyl-based structure, 20.

Only the torsion-angle data for 7-ring chelates 12 and 13 and 19 are incorporated in Figure 3. The larger chelate ring alters the geometry around Rh, so that one value of ϕ is larger and the other smaller than the 5-ring case. Overall, the range of variation in θ is greater for ψ -equatorial rings, with values for ψ -axial rings narrowly dispersed close to 0° .

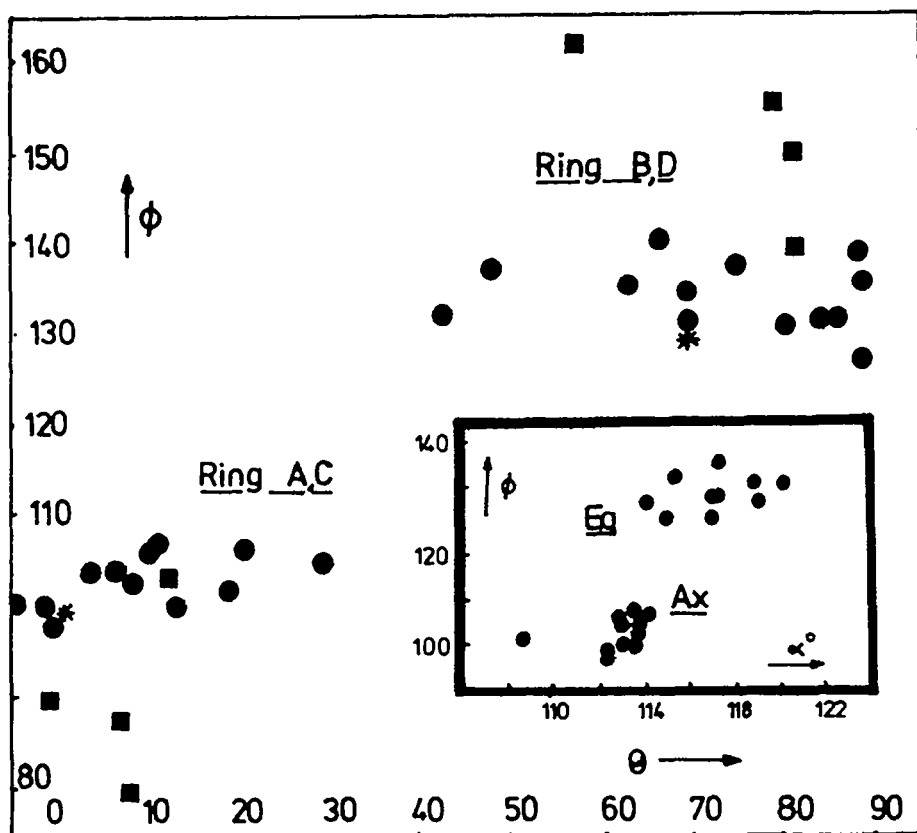


Figure 3 Relationship between torsion angles ϕ and θ , defined in the text. Structures 1, 2, 3, 5, 9 and 10 (5-ring chelates) are represented by \bullet and 12, 13 (7-ring chelates) by \blacksquare . The ideal 5-ring "edge-face" is represented by $*$. **Figure 5 (inset)**: relationship between torsion angle θ and RhPC bond angle for 5-ring chelates 1, 2, 5, 9 and 10; the P-axial and P-equatorial rings form distinct clusters.

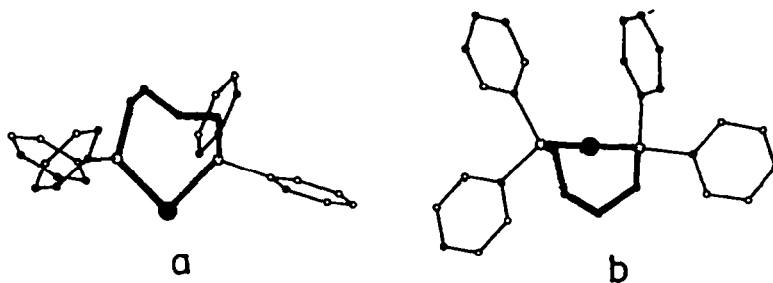


Figure 4 Plan (a) and elevation (b) views of the X-ray crystal of bis-diphenylphosphinobutane structure 17

Bond angles: The most symmetrical chiral phosphine complexes have a regular arrangement of P-aryl rings. With one exception, 9, the complexes are cationic and coordinatively unsaturated, permitting a favourable interaction between ortho C-H of aryl rings and the metal, orthogonal to the coordination plane. Such interactions are well recognised elsewhere¹⁵ as the beginning of an agostic interaction between metal and hydrogen. For the $14c$ complex (PPh_3), $Rh^+ ClO_4^-$, this interaction is sufficient to cause a 20° angular distortion of the trans PRHP array¹⁶.

For typical metal complexes ¹⁷ of $MePh_2P$, the MPC_{aryl} bond angles generally vary over the range $108-118^\circ$. If, in the series of chiral biphosphine complexes under scrutiny, the ψ -axial

ortho C-H's are involved in significant bonding to the metal, this should affect bond angles. Specifically, the angle $\text{RhPC}_{\text{aryl}}$ should be significantly smaller for ν -axial than for ν -equatorial rings. Figure 5 shows a plot of this angle (α) against the relevant torsion-angle (ϕ), for 5-ring chelates and reveals a systematic trend. The axial rings are clearly associated with smaller values of α . This accords with significant proximity of the relevant ortho-hydrogens to rhodium, typical values (derived from CHIRAPHOS complex (2)) being 2.68 Å and 2.90 Å. The 7-ring chelates do not reveal comparable trends.

Interaction between the P-aryl ring substituents and bound reactant governs the relative stability of diastereoisomeric intermediates in the catalytic cycle for asymmetric hydrogenation of enamides. This is now considered in detail.

2. Molecular Modelling of Dehydroamino acid Complexes

There are several crystal structures of metal complexes with a chelated enamide^{1a}; two of these are directly relevant to the pathway of asymmetric hydrogenation. In all of these the olefin and amide exhibit a near coplanar arrangement of M-O-C-N - C_α within the chelate ring with the second olefinic carbon C_β displaced out of this plane. The CHIRAPHOS complex 2 excited substantial interest since the olefinic face coordinated to rhodium is opposite to that expected from the stereochemical course of asymmetric hydrogenation. This result accords with the far higher reactivity of the DIPAMP enamide complex disfavoured at equilibrium towards H₂ at low temperatures^{1b}. The high energy diastereomer, which carries the flux of catalysis, has not been characterised crystallographically, nor has the initial dihydride product of H₂ addition been identified. For this reason, we carried out molecular modelling calculations to define the structural factors responsible for enantioselectivity.

Basis of the calculations: The CHEM3 molecular modelling programs provide a convenient method for assembling molecular structures from fragments made accessible by X-ray crystallography^{1a}. For transition-metal complexes this permits the reorientation of one ligand with respect to others, and the formation of new ligand-metal bonds, e.g. to hydrogen.

The steric energy of any given structure may in principle be calculated by molecular mechanics procedures. Unfortunately, the normal coordinate analyses necessary for deriving a suitable force-field are simply not available for rhodium complexes relevant to asymmetric hydrogenation. The structures concerned are rather rigid, and non-bonded interactions are most readily accommodated by rotation about single bonds, particularly the P-Ph units. This led to a simplified approach, in that the skeletal geometry was defined for a given structure, and the energy of van der Waals interaction then minimised by incremental rotation about conformationally mobile single bonds, making the further assumption that torsional barriers were not significant. This was carried out in the TORMIN subroutine of the COSMIC molecular modelling package (made available through the courtesy of Dr. J.G. Vinter, Smith, Kline and French^{1b}). This employs standard parameters for van der Waals interactions^{2c} and iterates to minimum energy. This iteration was continued until the energies derived in successive calculations converged to < 0.01 Kcal/mole⁻¹.

Enamide complexes: The X-ray crystal structure of (SS-CHIRAPHOS) (ethyl Z- α -acetamido-cinnamate) rhodium perchlorate, 2, has been reported; Table 1, reference (c). The data was modified by transformation into orthogonal coordinates with Rh at the origin, the phosphines in the xy plane, and the centrepoint of the chelate ring PCCP on the y axis. The ester ethyl group was excised and replaced by H, then hydrogen atoms were added at all relevant sites with a standard C-H distance of 1.08 Å^{1a}.

The van der Waals energy of this construct was then minimised with respect to rotation about the ten conformationally mobile single bonds^{1b}. Only slight structural changes occurred before a stable minimum was reached, and the total van der Waals energy decreased marginally to a value $\Delta H_0 = -31.3$ Kcal/mole⁻¹.

This structure was then changed from the C_α-re diastereomer into the C_α-si diastereomer by reflecting the dehydroamino acid fragment in the xy plane, thereby reversing the sign of all x

coordinates. A new van der Waals minimisation procedure was carried out by the same method, giving a final energy $\Delta H_0 = -29.3 \text{ Kcalismole}^{-1}$. The resulting structures are presented in Figure 6, indicating the regions where significant interactions occur. For the more stable C_{α} -re isomer, the only significant repulsion is between benzylidene C-H of enamide and ipso-carbon of adjacent arylphosphine. In contrast, the minor C_{α} -si diastereomer possesses several destabilising contacts.

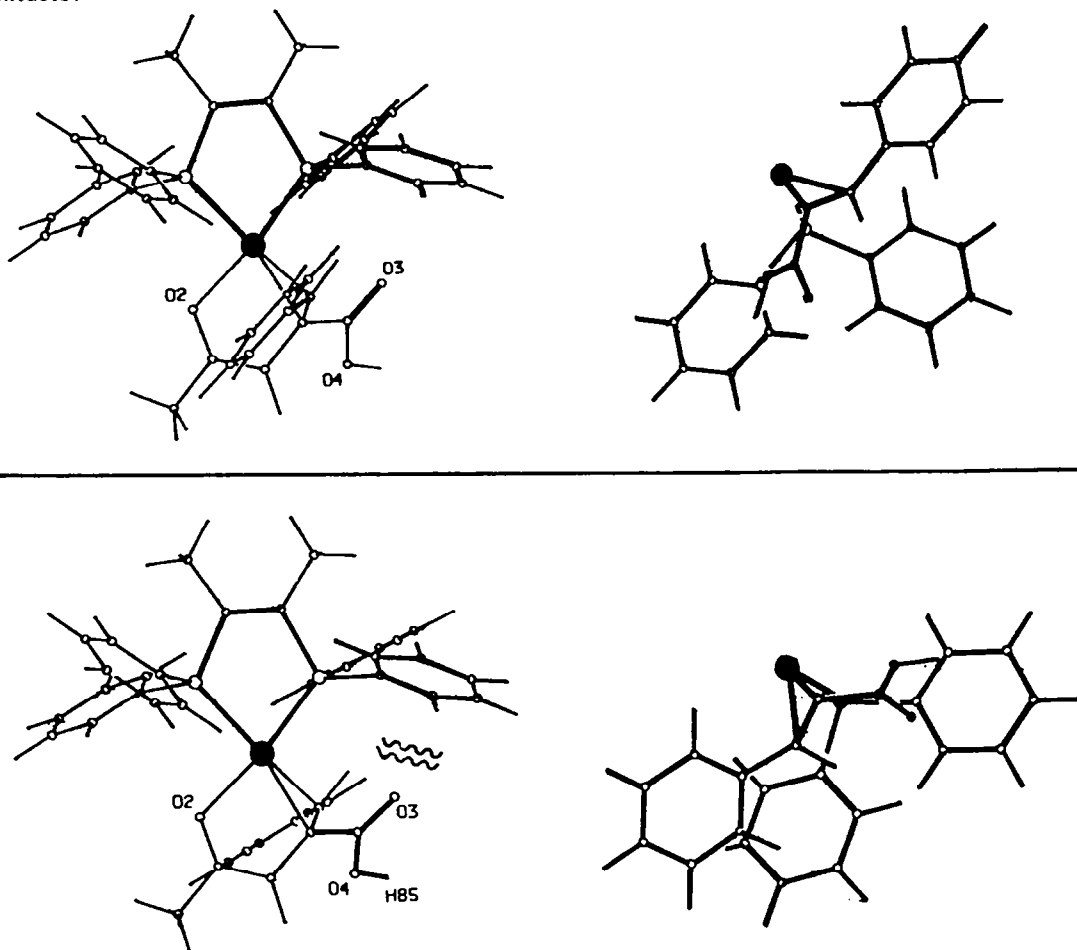


Figure 6 Minimum energy structures for CHIRAPHOS rhodium enamides from Z - α -PhCH = C(CO₂H)NHCOCH₃. Major diastereomer uppermost; right-hand view demonstrates interactions between the enamide and proximal PPh₂. For the minor diastereomer the region of unfavourable steric interaction between -CO₂H and P-Ph (eq) is highlighted.

The most significant of these involve the -CO₂H group and neighbouring equatorial P-arene group; the relative disposition of these two residues is such that steric repulsion cannot be greatly reduced by rotation about single bonds, without incurring greater cost elsewhere.

The difference in VdW interactions between the C_{α} -re and C_{α} -si diastereomers is quite small, well within the limits of accuracy of the method. Given this caution, it appears that the main difference in energy between major and minor enamide diastereomers in asymmetric hydrogenation resides in non-bonded interactions of the α -CO₂R group. Many publications support the idea that its presence is essential for a high optical yield, and if it is removed and replaced by H the E.e. is quite poor²⁰. Replacement of the α -CO₂R group in enol acetates by various substituted phenyl groups reduced the optical yield, substantially less so when the substituents were electron-withdrawing²¹.

Dihydride complexes: Addition of H₂ to a rhodium (or iridium) enamide complex leads directly to the corresponding alkylmetal hydride². Intermediacy of a dihydride is assumed, but not defined. Since [H₂] appears in the rate-equation^{2,22} and catalysis proceeds without equilibration of ortho and para-hydrogen²², it is the initial addition step rather than

intracomplex hydride-transfer which is rate-determining. This provides an incentive for studying models of the dihydrides in both stereochemical series to discover differential steric interactions.

Since the dihydrides are six-coordinate, each enamide complex can give rise to four diastereoisomeric products²³. These arise from four distinct pathways for H₂ addition; two above the square plane along the P-Rh-O and P-Rh-C vectors respectively and likewise two below the square-plane. Models of the four possible dihydrides were constructed from the minimised structure of the C_α-re isomer described in the previous section. In each case one of the Rh-P bonds was disconnected and the ligand then rotated through 90° about the remaining Rh-P bond. Two hydrogens were then added to rhodium at the vacant octahedral sites (Rh-H = 1.60 Å). The four resulting diastereomers were subjected in turn to minimisation of van der Waals energy, as previously described. In three cases very severe non-bonded interactions particularly between the C-Ph or C-CH₃ of the enamide chelate and adjacent -PPh₂, were incorporated which could not be relieved by torsional motion, giving rise to sterically impossible structures. The fourth isomer is still strained, but viable and is shown in Figure 7. This is the stereoisomer which would be expected to be on the hydrogenation pathway, with Rh-H in place for transfer to C_β.

An identical procedure was carried out for the less stable C_α-si enamide complex and again only one of the four stereoisomers has a low energy rotationally minimised structure, homologous to the one derived in the case of the C_α-re diastereoisomer (Figure 7). There is a striking difference in the relative energies of athe C_α-re (major) and C_α-si (minor) diastereomers, which are respectively +19.5 and -22.7 Kcalmole⁻¹, and the origin of such of this difference is apparent on inspection of Figure 7. Increased steric compression between the -CO₂H and adjacent -PPh₂ is responsible for the higher energy of the C_α-re isomer in Figure 7a. The aryl rings of that -PPh₂ are forced into close contact which distributes the destabilising interaction more widely. Further non-bonded interactions arise between the amide and the same PPh₂. Since steric compression is distributed over a substantial area of the complex, it cannot be relieved by torsional or twisting motions. In contrast, the C_α-si isomer shown in Figure 7b is relatively unencumbered, the main destabilising interaction involving a contact between Rh-H and an ortho-H of arylphosphine.

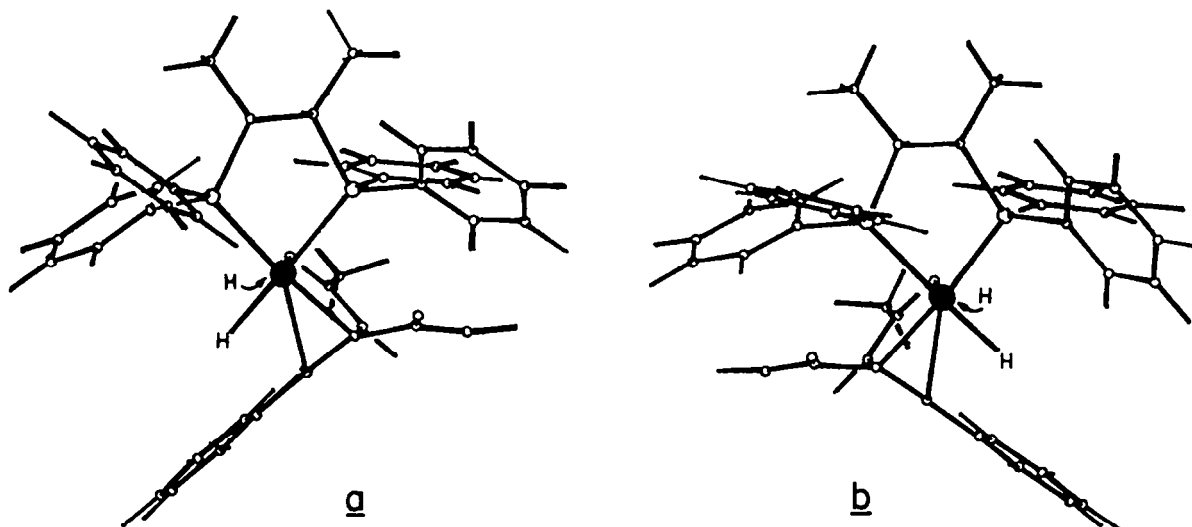


Figure 7 Minimised structures of the favoured Rh-diastereoisomers of enamide dihydrides, derived from the major (a) and minor (b) enamide complexes of Figure 6. In the former, serious non-bonded interactions occur between the CO₂H and equatorial P-Ph, the NHC(=O)CH₃, and axial P-Ph, and ortho-H of these two aryl rings. The latter, derived from the minor enamide is relatively uncrowded.

3. Reaction Pathway for H₂ addition

The energy surfaces for addition of H₂ to the enamide structures of Figure 6, along the vector leading to the dihydrides of Figure 7 was then studied. Several authors have carried out theoretical calculations on H₂ addition to metal complexes²⁰. Whilst parallel attack of H-H (with the two M-H distances kept equal throughout the reaction) is normally considered, both Dedieu and Strich, and Sevin have examined perpendicular H-H approach. Both groups concluded that a perpendicular trajectory was quite permissible in the early stages of reaction. However, the transition-state is late, and H₂ comes close to the metal before significant lengthening of the H-H bond occurs.

For molecular modelling studies, the relationship between H-H or Rh-H distances and distortion of ligand and substrate chelates out of the square-plane was derived from the work of Noell and Hay²¹. The H₂ molecule was positioned such that its mid point was located on the axis perpendicular to the square plane, with H-H parallel to P-Rh-O or P-Rh-C. This leads to four possible directions of H₂ approach, two above and two below the plane viewed in Figure 6. Only the one leading to a stable structure (vide supra) was studied in detail. For any given Rh-H distance, the biphosphine ligand was rotated out of the square plane about the P₂-Rh bond by the defined amount²² and the enamide ligand rotated out of plane to the same extent about Rh-C_α (see inset to Figure 8). This gives a structure corresponding to a point on the energy surface for H₂ addition, and the VdW interactions were calculated as before through the TORMIN routine, allowing all rotatable bonds to achieve a minimum conformation. The Rh-H distance was reduced by an increment, new skeletal geometry established for the ligands, and minimisation achieved as described. Three of these four lead to impossibly strained structures; only that with H-H parallel to P-Rh-O and approaching from the benzylidene face is sterically permitted. Figure 8 demonstrates how the VdW energy varies as the PRhO angle changes from 180° to 90°. A slight initial rise is succeeded by a region where little serious repulsion occurs. Only late in the reaction, when PRhO < 100°, does the level of non-bonded interaction increase dramatically. More detailed analysis of the changes in P-aryl torsion angles indicate that steric clashes are localised in one of the two pairs. Thus rings C and D change little in conformation whilst rings A and B fluctuate considerably as they endeavour to avoid the approach of the enamide residue.

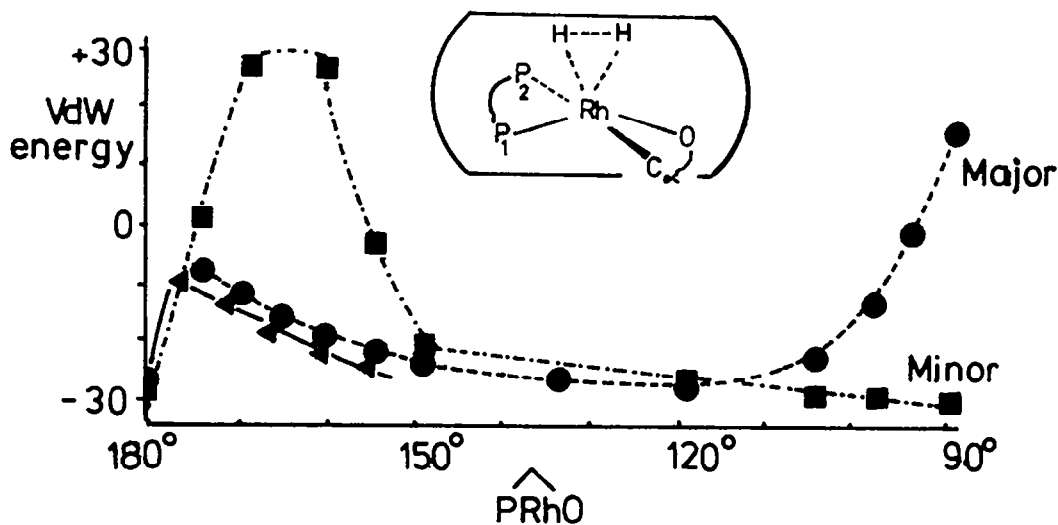


Figure 8 Van der Waals energy of computed intermediates in the H₂ pathway. ■ Minor diastereomer parallel addition ◄ minor diastereomer, perpendicular addition ● major diastereomer parallel addition (towards P-Rh-O).

The behaviour of the unstable enamide diastereomer (C_α-si) is in complete contrast, although again only one of the four pathways is sterically permissible. Here one observes serious steric interactions early in the H₂ addition process, essentially alleviated when the

PRhO angle is 150° , no further increase along the reaction profile. This prompted an examination of perpendicular H_2 approach during the initial phase of addition with other factors in the calculations unaltered. The results demonstrated in Figure 8 show that much, but not all, of the steric compression in the early stages has been avoided.

There is little experimental evidence against which these observations can be evaluated. The recent spate of η^2 -dihydrogen complexes might be considered to mimic an early point on the energy surface, but characterised examples²⁵ are formally derived from 5-coordinate precursors by addition of H_2 , so the analogy is poor. It may well be that the positioning of H_2 is relatively unconstrained in the initial stage of addition to the square-planar rhodium complex, so that the critical interactions, which determine the transition-state region, are those which occur later in the reaction when Rh-H bond formation is well-developed. This is in accord with the high reactivity of the C_α -si diastereomer and the discrimination which leads to enantioselectivity.

4. Relevance to the Mechanism of Asymmetric Hydrogenation

The work described here highlights the common features of asymmetric hydrogenation catalysts. We find that a probable contributor to the "edge-face" arrangement commonly found in crystal structures of rhodium biphosphine complexes is a weak interaction between P-axial ortho-hydrogens and the metal leading to slight RhPC angle differences between axial and equatorial aryl rings.

Using a simple molecular modelling approach, the difference in enthalpy between the stable C_α -re enamide and its C_α -si diastereomer is correctly predicted. Furthermore it can be seen that the destabilising interactions arise between the CO_2R group of dehydroamino acid and C_{ipso} or C_{ortho} , H_{ortho} of adjacent P-equatorial ring, for the C_α -si diastereomer. The stable C_α -re diastereomer has its CO_2R -group in an unconstrained region of space. On going to the corresponding enamide dihydrides, the steric energies are reversed. Of four diastereomers from each square-planar precursor only one is permissible on steric grounds; the others engender impossible clashes between ligand and substrate. For the favoured configuration, which has one Rh-H in place for transfer to the β -olefinic carbon along a stereoelectronically favourable pathway²⁶ the C_α -si diastereomer is strongly favoured whilst the C_α -re diastereomer suffers VdW repulsions. These are partly located in the region of the CO_2H group but much more widely distributed, and involve the amide methyl group as well now in the proximity of a P-aryl residue. The conclusion that the C_α -si diastereomer is favoured at the dihydride level is clear-cut.

Computer modelling of the reaction pathway for H_2 addition to the enamide complexes demonstrates the same destabilising interaction to be important in the late stages of reaction with $\text{PRhO} < 100^\circ$. In the early stages of reaction complications occur through repulsion of the incoming H_2 molecule, which are more severe for the C_α -si diastereomer if the approach vector is constrained. One important caveat must be introduced at this stage. In recent work²⁷ it was demonstrated that H_2 addition to a model iridium enamide complex lacking the $-\text{CO}_2\text{R}$ functionality occurs with clear stereochemical preference. The isomer formed under kinetic control with H_2 addition along the P-Ir-C reactor, is equivalent to one strongly disfavoured in these modelling studies although there is an equilibration process linking all possible diastereomers at -45°C . Until a closer model for the dihydride addition process has been examined experimentally, caution in the interpretation of these results is required.

Acknowledgements We thank: B.P. Research Centre Sunbury and S.E.R.C. for a CASE award (to PLE); Dr. A.R. Lucy made useful comments, Dr. J.G. Vinter, Dr. A. Davis and Dr. M. Saunders all made a substantial contribution to helping the molecular modelling studies, particularly in the initial phases, Professor J. Halpern, Professor A. Yamamoto, Dr. C.R. Landis and Dr. B. Heiser for providing X-ray structure data.

References

1. For example R. Noyori, M. Ohta, Y. Hsiao, M. Kitamura, T. Ohta and H. Takaya, J. Am. Chem. Soc., 108 (1986) 7117; R. Selke and H. Pracejus, J. Mol. Catal., 38, (1986) 213; U. Nagel, E. Kinzel, J. Andrade and G. Prescher, Chem. Ber., 119 (1986) 3326.

2. J. Halpern and C.R. Landis, J. Am. Chem. Soc., 109, (1987) 1746 ; J.M. Brown and P.J. Maddox, J. Chem. Soc. Chem. Commun., (1987) 1276.
3. J.M. Brown, P.A. Chaloner and G.A. Morris, J. Chem. Soc. Perkin II (1987) 1583.
4. (a) A.S.C. Chan and J. Halpern J. Am. Chem. Soc., 102 (1980) 838 ; (b) J.M. Brown and P.A. Chaloner, J. Chem. Soc. Chem. Commun., (1980), 344.
5. For the corresponding iridium enamide complexes, H₂ addition occurs rapidly but the first observable intermediate is an alkylhydride, even at low temperatures, N.W. Alcock, J.M. Brown and A.R. Lucy, J. Chem. Soc. Chem. Commun., (1985), 575.
6. H.B. Kagan in "Comprehensive Organometallic Chemistry" Vol 8, pg 463 ff. ; G. Wilkinson, F.G.A. Stone and E.W. Abel, Eds. Pergamon Press, 1982.
7. Both the Chicago and Oxford groups have expended considerable unpublished effort in this direction.
8. B.D. Vineyard, W.S. Knowles, M.J. Sabacky, G.L. Bachman and D.J. Weinkauff, J. Am. Chem. Soc., 99 (1977) 5946 ; W.S. Knowles, Acc. Chem. Res., 16 (1983) 106.
9. J.D. Oliver and D.P. Riley, Organometallics 2 (1983) 1032.
10. C.K. Prout, D.J. Watkin et al, Chemical Crystallography Laboratory, Oxford University.
11. K. Tani, T. Yamagata, S. Akutagawa, H. Kumabayashi, T. Taketomi, H. Takaya, A. Miyashita, R. Noyori and S. Otsuka, J. Am. Chem. Soc., 106 (1984) 5208, and refs therein.
12. V. Gramlich and C. Salomon, J. Organometal Chem., 73 (1974) C61 ; V. Gramlich and G. Consiglio, Helv. Chim. Acta. 62 (1979) 1016 ; R.G. Ball, B.R. James, J. Trotter, D.K. Wang and K.R. Dixon, J. Chem. Soc. Chem. Commun., (1979) 460 ; S. Brunie, J. Mazan, N. Langlois and H.B. Kagan, J. Organometal Chem., 114 (1976) 225 ; N.C. Payne and D.W. Stephan, J. Organometal Chem., 228 (1982) 203 ; D. Tranqui, A. Durif, M.N. Eddine, J. Lieto, J.J. Rafalko and B.C. Gates, Acta Cryst B 38 (1982) 1916.
13. G. Balavoine, S. Brunie and H.B. Kagan, J. Organometal Chem., 187 (1980) 125.
14. W.M.J. Flapper and C. Romers, Tetrahedron 31 (1975) 1705 ; D. F. Bocian and H.L. Strauss, J. Am. Chem. Soc., 99 (1977) 2876 ; A.L. Esteban, C. Galliano, E. Diez and F.J. Berjemo, J. Chem. Soc. Perkin 2 (1982) 657.
15. M. Brookhart and M.L.H. Green, J. Organometal Chem., 250 (1983) 395
16. Y.W. Yareol, S.L. Miles, R. Bau and C.A. Reed, J. Am. Chem. Soc., 99 (1977) 7076.
17. Inter alia N.W. Alcock and J.H. Nelson, Acta Cryst 41C (1985) 1748 ; F. Dahan and R. Choukroun Acta Cryst., 41C (1985) 704 ; H. Kin-Chee, G.M. McLaughlin, M. McPartlin and G.B. Robertson, Acta Cryst., 38 (1982) 421 ; J.C. Jeffrey, H. Razay and F.G.A. Stone, J. Chem. Soc. Dalton (1982) 1733 ; M.J. Chetcuti, K. Marsden, I. Moore, F.G.A. Stone and P. Woodward, J. Chem. Soc. Dalton (1982) 1749 ; A. Modinos and P. Woodward, J. Chem. Soc. Dalton (1975) 1534, 2134 ; M.A. Bennett, H-K. Chee and G.B. Robertson, Inorg. Chem., 18 (1979) 1061.
18. Table 1, ref c ; A.S.C. Chan, J.J. Pluth and J. Halpern, Inorg. Chim. Acta 37 (1979) C 477 ; N.W. Alcock, J.M. Brown and P.J. Maddox, J. Chem. Soc. Chem. Commun., 1986, 1532 ; A de Cian, R. Weiss, J-P. Haudegond, Y. Chauvin and D. Comereuc, J. Organometal Chem., 187 (1980) 73.
19. (a) CHEMX from Dr. K. Davies and associates, Molecular Design, Oxford (b) COSMIC and subroutines from Dr. J.G. Vinter, Smith Kline and French, Welwyn Garden City. For a similar approach to intermediates in hydrogenation by ClRh(PPh₃), see J.M. Brown, P.L. Evans and A.R. Lucy, J. Chem. Soc. Perkin II (1987) 1589.
20. J.M. Brown and D. Parker, Organometallics 1 (1982) 1350.
21. K.E. Koenig, G.L. Bachman and B.D. Vineyard, J. Org. Chem., 45 (1980) 2362.
22. J.M. Brown, L.R. Canning, A.R. Downs and A.M. Forster, J. Organometal Chem., 255, (1983), 103
23. P.A. MacNeil, N.K. Roberts and B. Bosnich, J. Am. Chem. Soc., 103 (1981) 2273.

24. J.J. Low and W.A. Goddard III, J.Am.Chem.Soc., 106 (1984) 6928 ; J.O. Noell and P.J. Hay, ibid, 104, (1982) 4578; S. Obara, K. Kitaara and K. Morokuma, ibid 106 (1984) 7482 ; N. Koga, C. Daniel, J. Han, X.Y. Fu and K. Morokuma, ibid 109 (1987) 3455; A. Dedieu, Topics in Physical Organometallic Chemistry 1 (1985) 1, and refs therein.
25. H.J. Wasserman, G.J. Kubas and R.R. Ryan, J.Am.Chem.Soc., 108, (1986) 2294; R.H. Crabtree, M. Lavin and L. Bonneviot, ibid 108 (1986) 4032 and refs. therein.
26. T.W. Dekleva and B.R. James, J.Chem.Soc.Chem.Commun., (1983) 1350.
27. J.M. Brown and P.J. Maddox, J.Chem.Soc.Chem.Commun., (1987) 1278.